colloids and interfaces

MDPI

Article

Exploring the Antifungal Effectiveness of a Topical Innovative Formulation Containing Voriconazole Combined with *Pinus sylvestris* L. Essential Oil for Onychomycosis

Safaa Halool Mohammed Al-Suwaytee [1,2], Olfa Ben Hadj Ayed [1], Raja Chaâbane-Banaoues [3], Tahsine Koksi [4], Maytham Razaq Shleghm [2], Leila Chekir-Ghedira [4], Hamouda Babba [3], Souad Sfar [1] and Mohamed Ali Lassoued [1,*]

[1] Laboratory of Pharmaceutical, Chemical and Pharmacological Drug Development (LR12ES09), Faculty of Pharmacy of Monastir, University of Monastir, Monastir 5000, Tunisia; safaa632658@gmail.com (S.H.M.A.-S.)
[2] Department of Pharmaceutics, College of Pharmacy, National University of Science and Technology, Thi-Qar 64001, Iraq
[3] Laboratory of Medical and Molecular Parasitology and Mycology (LR12ES08), Department of Clinical Biology B, Faculty of Pharmacy of Monastir, University of Monastir, Monastir 5000, Tunisia
[4] Laboratory of Natural Bioactive Substances and Biotechnology (LR24ES14), Faculty of Dental Medicine, University of Monastir, Avicenna Street, Monastir 5000, Tunisia
* Correspondence: mohamedali.lassoued@fphm.u-monastir.tn; Tel.: +216-98-24-98-58; Fax: +216-73-46-18-30

Abstract: (1) Background: The present study aimed to assess the antifungal effectiveness of a topical innovative formulation containing the association of an antifungal agent, voriconazole (VCZ), and the essential oil of *Pinus sylvestris* L. (PSEO). (2) Methods: Pseudo-ternary phase diagram and D-optimal mixture design approaches were applied for the development and the optimization of the o/w nanoemulsion. The optimized formulation (NE) was subjected to physicochemical characterization and to physical stability studies. In vitro permeation studies were carried out using the Franz cell diffusion system. The antimycotic efficacy against *Microsporum canis* was carried out in vitro. (3) Results: Optimal nanoemulsion showed great physical stability and was characterized by a small droplet size (19.015 nm ± 0.110 nm), a PDI of 0.146 ± 0.011, a zeta potential of −16.067 mV ± 1.833 mV, a percentage of transmittance of 95.352% ± 0.175%, and a pH of 5.64 ± 0.03. Furthermore, it exhibited a significant enhancement in apparent permeability coefficient ($p < 0.05$) compared to the VCZ free drug. Finally, NE presented the greatest antifungal activity against *Microsporum canis* in comparison with VCZ and PSEO tested alone. (4) Conclusions: These promising results suggest that this topical innovative formulation could be a good candidate to treat onychomycosis. Further ex vivo and clinical investigations are needed to support these findings.

Keywords: voriconazole; *Pinus sylvestris* L. essential oil; nanoemulsion; D-optimal mixture design; permeability; antifungal activity; *Microsporum canis*

Citation: Al-Suwaytee, S.H.M.; Ben Hadj Ayed, O.; Chaâbane-Banaoues, R.; Koksi, T.; Shleghm, M.R.; Chekir-Ghedira, L.; Babba, H.; Sfar, S.; Lassoued, M.A. Exploring the Antifungal Effectiveness of a Topical Innovative Formulation Containing Voriconazole Combined with *Pinus sylvestris* L. Essential Oil for Onychomycosis. *Colloids Interfaces* **2024**, *8*, 56. https://doi.org/10.3390/colloids8050056

Academic Editor: Reinhard Miller

Received: 21 August 2024
Revised: 9 October 2024
Accepted: 14 October 2024
Published: 17 October 2024

1. Introduction

Fungal infections pose a significant threat to public health. They can vary in severity and manifest in different clinical forms, ranging from superficial to systemic infections [1]. Cutaneous fungal infections affect around 20–25% of people globally [2]. Onychomycosis (*Tinea ungium*) is an extremely common and contagious nail unit fungal infection observed in clinical practice, which accounts for up to 50% of nail infections. Approximately 10% of the global population is afflicted with this disorder. Age, diabetes, immunosuppression, hyperhidrosis, obesity, tinea pedis, contacts with fungal diseases, and direct trauma to the nail are some risk factors [3]. Onychomycosis causes aesthetic and functional issues with the nail, such as thickening, yellow or white discoloration, distortion, separating the nail from the nail bed, and other nail abnormalities [2,3]. Fungal nail infections are mostly resulting from dermatophytes (60% to 70% of cases) (*Epidermophyton floccosum*, *Trichophyton rubrum*,

Trichophyton mentagrophytes, and *Microsporum canis*), non-dermatophytes molds, and yeast (particularly *Candida albicans*) [2,4]. The treatment of onychomycosis is challenging, and occurrences of relapse and reinfection are very common [5].

Antifungal agents can be applied either topically or used orally. Mild to moderate cases of nail fungus are generally treated topically using nail lacquers (ciclopirox 8%, amorolfine 5%) or topical solutions (efinaconazole 10%, tavaborole 10%), while moderate to severe onychomycosis cases are typically managed with oral antifungal medications using griseofulvin, terbinafine, and azoles (itraconazole, fluconazole, and ketoconazole) [3,6–8].

Terbinafine and itraconazole are considered the gold standard of oral treatment; however, resistant cases of onychomycosis and poor responses to those traditional antifungals have been reported recently [3,8,9]. In this context, new antifungal agents, including voriconazole (VCZ), may play a significant role to overcome this threat regarding antifungal resistance [6,8–10].

VCZ, a synthetic second-generation triazole, is commercially available as oral (tablets and oral suspensions) and intravenous formulations [11]. It is indicated, in adults and pediatric patients, to treat invasive aspergillosis, disseminated candidiasis, candidaemia in non-neutropenic patients, and severe fusarium and scedosporium fungal infections [12]. Furthermore, this broad-spectrum antifungal agent has proven efficacy against the more common fungal pathogens [13,14].

Antifungal medications administered orally require an extended treatment period to achieve a complete nail cure and pose a risk of serious adverse effects (hepatotoxicity, gastrointestinal disorder, etc.), as well as drug interactions [3,15].

The use of topical treatments offers the benefit that they minimize the risk of systemic side effects and thus ensure higher patient compliance since they target, directly, the site of infection [16]. However, the efficacy of a topical antifungal agent is largely dependent on its passage at an effective concentration through the nail barrier, which is characterized by its limited permeability to molecules due to its structure (several layers of compacted keratinized cells) [17]. Numerous strategies have been developed to improve drug permeation through the nail plate, including the use of o/w nanoemulsions [18].

In the past few years, essential oils (EOs) have gained significant attention as natural and affordable substitutes or as complements to traditional antifungal medications [19,20]. In addition, because EOs are complex mixtures of organic compounds, the possibility of microbial resistance to this combination of chemicals is lower than that of a single target [21]. Moreover, several published studies highlighted the synergistic effect of essential oils in combination with antifungal agents against fungal pathogens such as dermatophytes and yeasts [22–25].

This current study aimed to develop and characterize an innovative formulation (o/w nanoemulsion) with *Pinus sylvestris* L. essential oil (PSEO) and VCZ for topical application and to explore its antifungal effectiveness compared to the two compounds used alone. According to our best knowledge, there are few published studies that discuss the antifungal activity of *Pinus sylvestris* L. essential oil (PSEO) [23,26], as well as the synergistic antifungal effect of essential oils or terpenoid compounds with voriconazole [27,28]. Furthermore, there are no previous works that described the investigation of the potential synergetic effectiveness of the combination of VCZ-PSEO formulated into an o/w nanoemulsion for the topical treatment of onychomycosis.

2. Materials and Methods

2.1. Drug and Chemical Reagents

Voriconazole pharmaceutical grade (VCZ) was a gift from Philadelphia Pharma laboratories (Sfax, Tunisia). *Pinus Sylvestris* L. essential oil (PSEO) was bought from Parachimic (Sfax, Tunisia). Corn oil was purchased from a local market. Diethylene glycol monoethyl ether (Transcutol® HP) was obtained from Gattefossé SAS (Saint-Priest, France). Polyoxyl 35 hydrogenated castor oil (Kolliphor® EL) and Sorbitane Monooleate (Span® 80) were

supplied from Sigma-Aldrich Chemie (Steinheim, Germany) and LobaChemie (Mumbai, India), respectively. All other reagents or solvents used were of analytical grade.

2.2. Formulation of VCZ-Based Nanoemulsion

2.2.1. Selection of the Oily Phase Components

Corn oil, Transcutol® HP, Kolliphor® EL (HLB value = 12–14), and Span® 80 (HLB value = 4.3) were used as solvent, cosolvent (CoS), surfactant, and cosurfactant, respectively. These excipients were selected for their compatibility, their ability to form stable o/w nanoemulsions, and their safety toward skin tissues [29–31]. PSEO was chosen, based on the literature, due to its proven antifungal properties [23,26,32,33].

2.2.2. Pseudo-Ternary Phase Diagrams

Pseudo-ternary phase diagrams were constructed to determine the concentration ranges of the oily phase components that delimit the nanoemulsion area.

Corn oil and PSEO (oil mixture) were used with a constant ratio of 1:1 (*wt*/*wt*) across all diagrams. Kolliphore® EL and Span® 80 (Smix) were kept constant at a ratio of 5:1 (*wt*/*wt*). Smix/CoS were tested at different weight ratios (1:1, 3:1, 5:1; *wt*/*wt*).

Pseudo-ternary phase diagrams were prepared using the water titration method by varying the ratio of corn oil/PSEO and Smix/CoS from 1:9 to 9:1 (*wt*/*wt*). For each combination, water was added dropwise to the oily phase under moderate magnetic stirring (250 rpm) at room temperature until a milky white emulsion appeared. The region of nanoemulsion was established using ProSim® Ternary Diagram software (version 1.0.2, Labège, France). The pseudo-ternary diagram that exhibited the largest nanoemulsion area was chosen for the optimization step.

2.2.3. Nanoemulsion Optimization Using D-Optimal Mixture Design

D-optimal mixture design was chosen in order to optimize the nanoemulsion formulation. Three variables, expressed in percentage, were designated as the independent factors in the experimental design, viz., Smix/CoS amount (A, % *wt*/*wt*), water amount (B, % *wt*/*wt*), and corn oil/PSEO amount (C, % *wt*/*wt*). The low and high levels of each independent variable (Table 1) were fixed according to the results obtained from the selected pseudo-ternary phase diagram. Droplet size (Y_1) and polydispersity index (PDI) (Y_2) were defined as responses to assess and optimize the characteristics of the formulated nanoemulsion.

Table 1. D-optimal mixture design: independent and dependent variables.

Independent Variables	**Predefined Levels**	
	Low (–1)	**High (+1)**
A: percentage of Smix/CoS (% *wt*/*wt*)	15	25
B: percentage of water (% *wt*/*wt*)	70	80
C: percentage of corn oil/PSEO (% *wt*/*wt*)	3	8.5
Dependent Variables	**Goals**	
Y1: droplet size (nm)	Minimize	
Y2: polydispersity index (PDI)	Minimize	

Statistical analysis was conducted using the Design Expert® software (Version 12, Stat-Ease Inc., Minneapolis, MN, USA). Sixteen experimental runs were generated by the experimental design software (Figure S1—Supplementary Materials; Table 2): eleven experiments to develop the predictive model and five replicated experiments in the center of the domain to estimate the experimental error. Analysis of variance (ANOVA) was used to determine the best fitting mathematical model to establish the polynomial equation for each response (Y_1 and Y_2).

Table 2. Experimental matrix of the mixture design and observed results of each response.

Run	A	B	C	Y1	Y2
1	17.87	79.13	3.00	14.63	0.140
2	19.75	74.75	5.50	14.62	0.146
3	19.75	74.75	5.50	15.02	0.128
4	19.75	74.75	5.50	15.34	0.140
5	25.00	70.00	5.00	14.47	0.130
6	15.00	76.50	8.50	52.83	0.657
7	19.75	74.75	5.50	16.10	0.103
8	17.52	74.73	7.75	28.75	0.331
9	19.75	74.75	5.5	16.13	0.122
10	17.16	77.22	5.62	17.39	0.121
11	24.40	72.60	3.00	13.69	0.157
12	15.00	80.00	5.00	17.68	0.138
13	22.10	72.30	5.60	15.42	0.128
14	21.50	70.00	8.50	26.72	0.432
15	20.55	76.45	3.00	15.09	0.183
16	19.63	72.44	7.93	23.53	0.354

A: percentage of Smix/CoS (% *wt*/*wt*); **B:** percentage of water (% *wt*/*wt*); **C:** percentage of corn oil/PSEO (% *wt*/*wt*); **Y1:** particle size (nm); **Y2:** polydispersity index (PDI).

The selection of the appropriate mathematical model among those under consideration (linear, quadratic, special cubic, and cubic models) was based on the comparison of different statistical parameters, viz., the sequential *p*-value, the lack of fit *p*-value, the standard deviation, the squared correlation coefficient (R^2), the adjusted R^2 and the predicted R^2, and the predicted residual sum of square (PRESS). Ultimately, the desirability function of the Design Expert® software was utilized to optimize the three independent variables (A, B, and C) and determine the optimal nanoemulsion formulation according to the following two criteria: (1) maximizing the amount of oily phase in order to encapsulate the highest amount of voriconazole, and (2) minimizing the droplet size (Y_1) and the PDI (Y_2) to ensure great stability of the formulation and improve voriconazole transport across the nail barrier.

2.3. Preparation of the Optimized Nanoemulsion

The preparation of the optimal nanoemulsion loaded with 1% (*wt*/*wt*) of VCZ was as follows: first, the oily phase (corn oil + PSEO + Transcutol® HP + Kolliphor® LE + Span® 80) was prepared by mixing all the components together at room temperature under gentle magnetic stirring (250 rpm) for 5 min. Next, the appropriate amount of VCZ was added to the previous blend and mixed under the same stirring conditions (250 rpm, at room temperature) until the drug was completely dissolved. Finally, the required amount of distilled water was added dropwise, and the preparation was mixed until a translucent nanoemulsion was obtained.

2.4. Physicochemical Characterization of the Optimal VCZ-Loaded Nanoemulsion

2.4.1. Droplet Size, PDI, and Zeta Potential Determination

Droplet size, expressed in nm, and polydispersity index (PDI) were measured at 25 °C after a dilution to tenth (*v*/*v*) in distilled water, using a Nanosizer® instrument (Nano-S, Malvern Instruments, Malvern, UK). Results were expressed as mean ± standard error of three repetitions (n = 3).

Zeta potential was determined using a Zetasizer® instrument (Nano-Z, Malvern Instruments, UK) at 25 °C after dilution to the hundredth (*v*/*v*) in double distilled water. The measurements were performed in triplicate (n = 3), and results were expressed in mV as mean ± standard error.

2.4.2. Percentage of Transmittance

The transparency of the optimal formulation was evaluated at room temperature using a UV–visible spectrophotometer (Thermo Scientific® Evolution 60, Madison, WI, USA) [34].

Measurements were carried out at 650 nm after a dilution to tenth (v/v) in distilled water (the latter was used as the reference). Results were expressed, in percentage (%), as mean ± standard error of three repetitions (n = 3).

2.4.3. pH Measurement

pH determination was performed in triplicate (n = 3), at room temperature, using a Thermo Orion® 410 (Thermo Scientific®, Waltham, MA, USA) pH meter [34]. Results were expressed as mean ± standard error.

2.5. Stability Studies

2.5.1. Stability to Centrifugation

A total of 2 ml of the optimized nanoemulsion was transferred into an Eppendorf tube and centrifuged at room temperature at 14,000 rpm for 20 min using a Hettich Mikro® 120 Centrifuge (Tuttlingen, Germany). Next, the preparation was visually checked for possible instabilities (phase separation, VCZ precipitation, etc.).

2.5.2. Stability to Temperature Cycles

Three heating–cooling cycles of 48 h each were performed, alternating 24 h at +45 °C and 24 h at +4 °C. The sample was then visually inspected for any sign of instability [34].

2.5.3. Stability to Freeze–Thaw Cycles

The optimal nanoemulsion underwent 3 freeze–thaw cycles of 48 h each, alternating 24 h at −21 °C and 24 h at +25 °C. The preparation was then subject to a visual inspection for any sign of instability [34].

2.6. In Vitro Cytotoxicity Assay

2.6.1. Cell Culture

HacaT cells were cultured in Dulbecco's modified Eagle's medium (DMEM) supplemented with 10% fetal bovine serum (FBS) and antibiotics (Gentamycin). Cells were maintained at 37 °C in a humidified atmosphere with 5% CO_2.

2.6.2. Cell Viability Assay

HacaT cells (10^4 cells/well in 100 µL medium) were seeded in 96-well plates and incubated for 24 h. Cells were, then, treated with different concentrations of VCZ, VCZ-loaded nanoemulsion (NE-VCZ), and unloaded nanoemulsion (NE-Blank) (50, 25, 12.5, 6.25, 3.125, 1.56 µg/mL) for 48 h. The MTT assay, a colorimetric test, was utilized to determine cell viability. The test measures the ability of living cells to reduce a tetrazolium salt, 3-(4,5-dimethylthiazol-2-yl)-2,5-diphenyltetrazolium bromide, due to the presence of mitochondrial succinate dehydrogenases. Cells were exposed to 40 µL of MTT (1 mg/mL) for 3 h at 37 °C in the appropriate complete medium. The medium was then discarded, and the formazan blue formed in the cells was solubilized by adding 100 µL DMSO. Negative control without the tested molecules was prepared in the same manner. Optical density (OD) was measured at 570 nm.

The viability percentage was ultimately calculated using Equation (1):

$$\text{Viability}(\%) = \left(\frac{\text{OD test}}{\text{OD control}}\right) \times 100 \quad (1)$$

with **OD test:** absorbance of the tested molecule and **OD control:** absorbance of the negative control.

Results were represented as the mean ± standard deviation (SD) of three experiments (n = 3). Statistical analyses were conducted using GraphPad Prism® software (version 8.0.2, GraphPad Software Inc., La Jolla, CA, USA) using a two-way analysis of variance (ANOVA), followed by Tukey's multiple comparison test. Statistical significance was assigned at p value <0.05.

2.7. In Vitro Drug Permeation Studies

In vitro permeation studies of the voriconazole free drug (suspension) versus the VCZ-loaded nanoemulsion were performed using a Franz diffusion cell system. The latter consists of a donor (upper part) and a receiver (lower portion) compartments separated by a dialysis membrane (MD34 1M; 7000D MwCO; Spectrum Laboratories, Rancho Dominguez, CA, USA) (Figure S2—Supplementary Materials).

The donor chamber contains 1 g of the sample to test (1% (*wt*/*wt*) of VCZ dispersed in distilled water or the optimized nanoemulsion loaded with 1% (*wt*/*wt*) of VCZ). The receiver chamber is filled with 5.4 mL of a mixture of pH 7.4 phosphate buffer solution (PBS) and ethanol absolute prepared at a ratio of 3:1 (*v*/*v*). The dialysis membrane is cut into small discs, inserted between the two compartments, and held in place using a clamp.

The Franz cell system was maintained, during the experiment, at a temperature of 32 ± 0.5 °C under a magnetic stirring rate of 250 rpm (Figure S3—Supplementary Materials).

The samples to be tested were added to the donor compartment and, at determined time intervals (30 min; 1 h; 2 h; 3 h; 4 h; 6 h), all the receptor compartment was withdrawn, filtered through a 0.45 µm filter, and spectrophotometrically assayed at 256 nm using a UV spectrophometer (Thermo Scientific® Evolution 60, USA). Moreover, the receiver compartment was immediately refilled with the same amount of fresh receiver medium. Results were expressed, in percent, as mean values ± standard error of three determinations (n = 3).

To compare the diffusion profiles of the VCZ free drug versus the optimized nanoemulsion, a model-independent approach using difference factor (f_1) and similarity factor (f_2) was employed [35]. f_1 and f_2 calculate the difference and similarity in percent between the two curves at each time point, respectively.

f_1 and f_2 were determined according to Equations (2) and (3), respectively.

$$f_1 = \left\{ \frac{\sum_{t=1}^{n} |R_t - T_t|}{\sum_{t=1}^{n} R_t} \right\} \times 100 \quad (2)$$

$$f_2 = 50 \times \log \left\{ \left[1 + \frac{1}{n} \sum_{t=1}^{n} (R_t - T_t)^2 \right]^{-0.5} \times 100 \right\} \quad (3)$$

with **n:** number of time points, $\mathbf{R_t}$: diffusion value of the reference (free drug) at time t, and $\mathbf{T_t}$**:** diffusion value of the optimal nanoemulsion at time t.

The diffusion profiles of the VCZ free drug versus the VCZ nanoemulsion are considered similar if the f_1 value is less than 15% and the f_2 value is higher than 50%.

The apparent permeability coefficients (P_{app}) were calculated according to Equation (4) [36]:

$$P_{app} = \frac{dQ}{dt} \times \frac{1}{AC_0} \quad (4)$$

where $\mathbf{P_{app}}$ (cm/s) is the apparent permeability coefficient, **A** (2.01 cm^2) is the effective surface area of the dialysis membrane exposed to the two chambers, $\mathbf{C_0}$ (µg/mL) is the initial concentration of the drug in the donor compartment, and **dQ/dt** (µg/s) is the amount of drug permeated per unit of time.

Data statistical analysis was carried out using Microsoft Office® Excel software (version 2016, Microsoft Inc., Redmond, WA, USA). Student's *t*-test was used to compare P_{app} mean values of VCZ suspension versus the optimized nanoemulsion. The difference observed between the two groups was considered significant when p-value ≤ 0.05.

2.8. In Vitro Antifungal Activity

2.8.1. Fungi Strains

The antifungal efficacy of the optimized VCZ-loaded nanoemulsion was tested on a dermatophyte clinical strain, *Microsporum canis* (MS 8972), which was isolated from nails with confirmed onychomycosis diagnostic (local Myco collection, Laboratory of

Parasitology and Mycology of the Fattouma Bourguiba University Hospital in Monastir, Tunisia). The fungal strain was maintained on Sabouraud Dextrose Agar (SDA) medium.

2.8.2. Disk Agar Diffusion Assay

A hyphal suspension from a ± 21days dermatophytes culture was utilized to infect Muller–Hinton agar (MHA) plates with 2% glucose. After adjusting the solution to 106 VU/mL, the plates were permitted to air dry for 20 min. Next, 5 µL of voriconazole suspension (VCZ-SUSP), *Pinus sylvestris* essential oil (PSEO), VCZ-loaded optimal nanoemulsion (NE-VCZ), and unloaded nanoemulsion (NE-Blank) were added to Whatman® grade 1 filter paper 6 mm disks. Disks had been placed in the middle, and MHA plates were infected. Subsequently, the plates were kept in an incubator at 28 °C for three to seven days. As soon as mycelium growth became apparent, the sizes of the inhibition zone diameters (IZDs) surrounding the antifungal disks were measured [37].

Results of the inhibition zone diameter were expressed, in mm, as mean values ± standard error of three determinations (n = 3).

3. Results

3.1. Formulation and Optimization of VCZ-Loaded Nanoemulsion

3.1.1. Pseudo-Ternary Phase Diagrams

Three pseudo-ternary phase diagrams were established using Kolliphore® EL and Span® 80 (Smix) as surfactant and cosurfactant, respectively, and Transcutol® HP as co-solvant (CoS) (Figure 1). Smix/CoS were blended at different weight ratios (Figure 1a = 1:1 (*wt*/*wt*); Figure 1b = 3:1 (*wt*/*wt*); and Figure 1c = 5:1 (*wt*/*wt*)). As can be seen, an enlargement in the nanoemulsion region was observed when the proportion of Kolliphore® EL/Span® 80 increased in the Smix/CoS blend from 1:1 (*wt*/*wt*) to 5:1 (*wt*/*wt*). Thus, the pseudo-ternary phase diagram obtained using the Smix/CoS ratio of 5:1 (*wt*/*wt*) was retained for the optimization step.

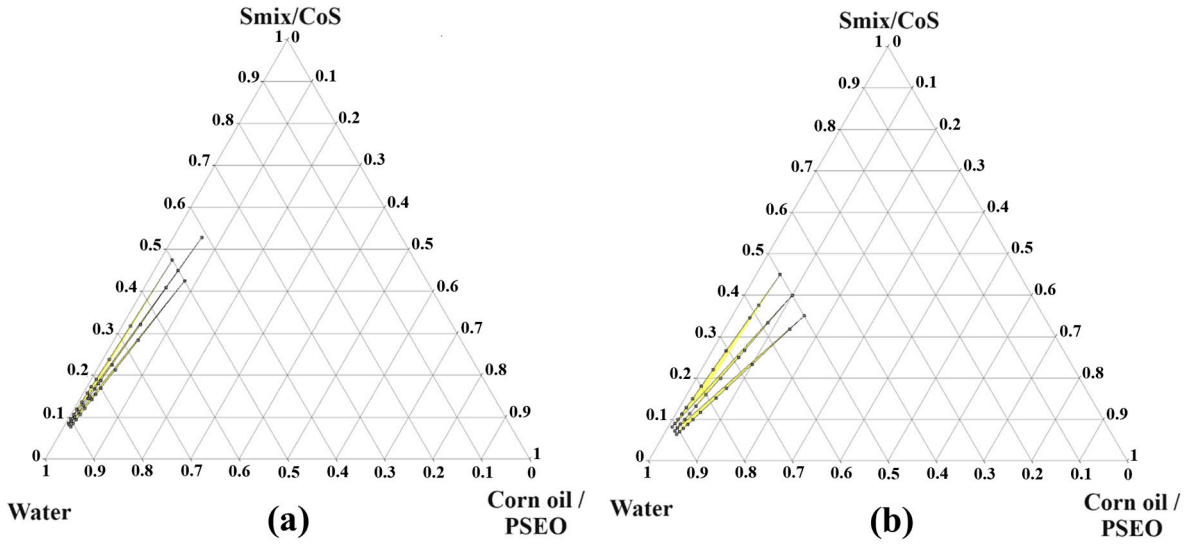

Figure 1. *Cont.*

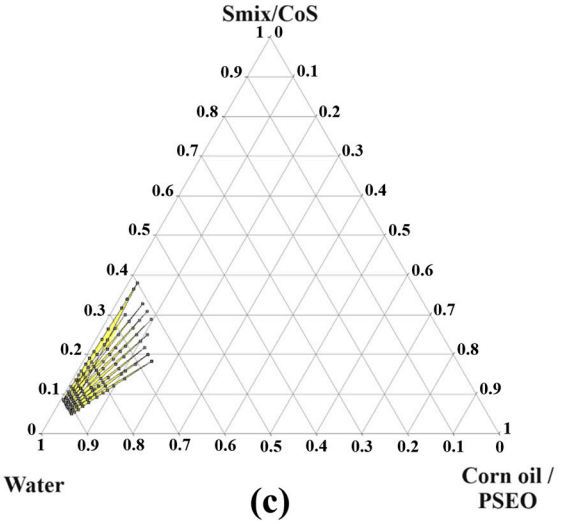

Figure 1. Pseudo-ternary phase diagrams showing the nanoemulsion area composed of corn oil/PSES (1:1; *wt*/*wt*) as an oil mixture, Kolliphore® EL (surfactant)/Span® 80 (cosurfactant) (5:1; *wt*/*wt*) as Smix, Transcutol® HP as a cosolvent (CoS), and distilled water as a dispersant. Smix/CoS are tested at three different weight ratios: (**a**) (1:1; *wt*/*wt*), (**b**) (3:1; *wt*/*wt*), and (**c**) (5:1; *wt*/*wt*).

3.1.2. Experimental Design

A D-optimal mixture design was performed for the optimization of the nanoemulsion. The percentages of the three components, viz., Kolliphore®EL/Span®80/Transcutol HP® (A), water (B), and corn oil/PSEO (C), were used as the independent factors. As seen in Table 1, the low and high levels for A, B, and C were 15–25%, 70–80%, and 3–8.5%, respectively.

Droplet size (Y_1) and PDI (Y_2) were defined as responses. The macroscopic aspect of the 16 experimental points generated by Design Expert® software is depicted in Figure S4 (Supplementary Materials). Droplet size and PDI are reported in Table 2. As seen, the droplet size of the 16 runs was below 100 nm and ranged from 13.69 nm to 52.83 nm. Their PDI values were between 0.103 and 0.657.

Y_1 and Y_2 responses were analyzed using the experimental design software to determine the best-fitting mathematical model and to calculate its coefficients. According to the results of the statistical analysis provided by Design-Expert® software (Tables S1 and S2—Supplementary Materials), the cubic model was retained for both responses (droplet size and PDI), since it presented the lowest standard deviation (0.7714 and 0.0174 for Y_1 and Y_2, respectively), PRESS values (151.45 and 0.049 for Y_1 and Y_2, respectively), and the highest squared correlation coefficient (R^2) (0.9976 and 0.9949 for Y_1 and Y_2, respectively) among the other models under consideration. Moreover, for both responses, the sequential *p*-values (0.0009 and 0.0413, for Y_1 and Y_2, respectively) were significant (<0.05), and the lack of fit *p*-values (0.2460 and 0.3849 for Y_1 and Y_2, respectively) were not significant (>0.05). Finally, the difference between the adjusted R^2 (0.9939 and 0.9871 for Y_1 and Y_2, respectively) and the predicted R^2 (0.8972 and 0.8614 for Y_1 and Y_2, respectively) was less than 0.2, indicating a good fit of the cubic model.

The cubic model for Y_1 (droplet size) is represented by Equation (5) as follows:

$$\begin{aligned} Y_1 = &-7613.45 \times \text{Smix/CoS} - 76.8327 \times \text{Water} + 353{,}766 \times \text{Corn Oil/PSEO} \\ &+ 12{,}779.5 \times \text{Smix/CoS} \times \text{Water} - 568{,}362 \times \text{Smix/CoS} \times \text{Corn Oil/PSEO} \\ &- 541{,}471 \times \text{Water} \times \text{Corn Oil/PSEO} + 389{,}224 \times \text{Smix/CoS} \times \text{Water} \\ &\times \text{Corn Oil/PSEO} + 5042.11 \times \text{Smix/CoS} \times \text{Water} \times (\text{Smix/CoS-Water}) \\ &+ 290{,}210 \times \text{Smix/CoS} \times \text{Corn Oil/PSEO} \times (\text{Smix/CoS-Corn Oil/PSEO}) \\ &+ 192{,}047 \times \text{Water} \times \text{Corn Oil/PSEO} \times (\text{Water-Corn Oil/PSEO}) \end{aligned} \quad (5)$$

The cubic model for Y_2 (PDI) is represented by Equation (6) as follows:

$$\begin{aligned} Y_2 = &-210.813 \times \text{Smix/CoS} + 2.16032 \times \text{Water} + 5422.1 \\ &\times \text{Corn Oil/PSEO} + 366.141 \times \text{Smix/CoS} \times \text{Water} - 8538.69 \times \text{Smix/CoS} \\ &\times \text{Corn Oil/PSEO} - 8329.47 \times \text{Water} \times \text{Corn Oil/PSEO} + 6010.28 \times \text{Smix/CoS} \\ &\times \text{Water} \times \text{Corn Oil/PSEO} + 191.341 \times \text{Smix/CoS} \times \text{Water} \times (\text{Smix/CoS-Water}) \\ &+ 4048.7 \times \text{Smix/CoS} \times \text{Corn Oil/PSEO} \times (\text{Smix/CoS-Corn Oil/PSEO}) \\ &+ 2934.39 \times \text{Water} \times \text{Corn Oil/PSEO} \times (\text{Water-Corn Oil/PSEO}) \end{aligned} \quad (6)$$

To study the effect of Smix/Cos, water, and corn oil/PSEO on the droplet size and the PDI of VCZ-loaded nanoemulsion, a Cox response trace plot was used (Figure 2).

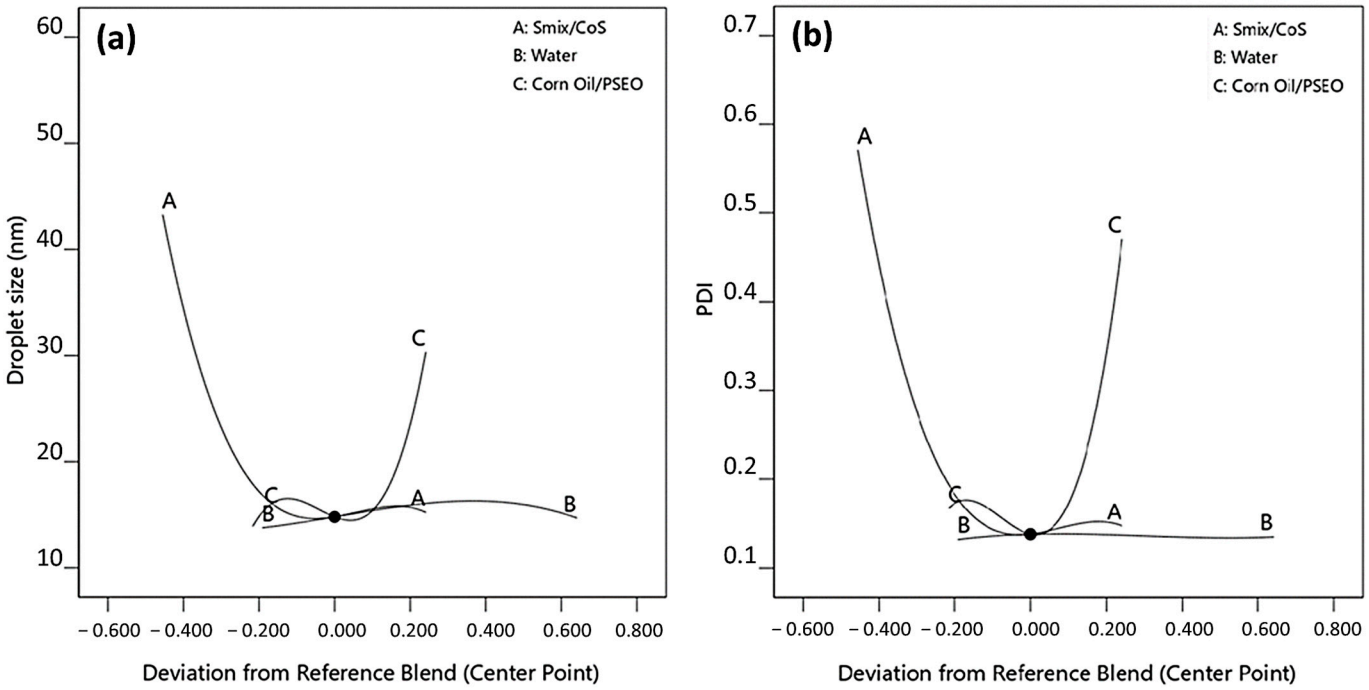

Figure 2. Cox response trace plot of (**a**) droplet size (Y1) and (**b**) PDI (Y2) responses.

According to Figure 2a, an increase in corn oil/PSEO (C) amount from 3% to 8.5% led to a significant raise in droplet size. In contrast, an increase in Smix/CoS (A) percentage from 15% to 25% resulted in a significant decrease in the droplet size. Same tendencies were observed for the PDI (Figure 2b), with an increase in this response when the amount of oil mixture (C) increased and a decrease in its value when the percentage of Smix/CoS (B) increased in the formulation. Finally, for both responses (Y1 and Y2), water (B) exhibited the less pronounced curve among the other studied components when varying from 70% to 80%, which indicates that the latter has a slight impact on droplet size and PDI.

The desirability function was utilized in optimizing the nanoemulsion formulation. The optimization aimed to minimize both responses Y_1 (<100 nm) and Y_2 (<0.3) and to maximize the percentage of corn oil/PSEO as well as that of Smix/CoS. Design-Expert® software provided a unique solution taking into account the different criteria cited above. The proposed optimal formulation was composed of 6.69% oil mixture, 23.31% Smix/CoS, and 70% water. The predicted droplet size and PDI values for the optimized nanoemulsion were 13.99 nm and 0.152, respectively, with a good desirability value (0.842). With the aim of validating the predicted values of both responses, the given formulation by the software was prepared and assessed for droplet size and PDI. Results were 14.49 nm ± 0.04 nm and 0.182 ± 0.010 for Y1 and Y2, respectively. According to the results of the statistical analysis generated by Design-Expert® software (Table 3), the proposed optimal formulation was validated. Thus, it was adopted for further studies.

Table 3. Results of the statistical analysis for the validation of the predicted responses (Design-Expert® software).

Solution 1 of 1 Response	Predicted Mean	Predicted Median	Std Dev	SE Pred	95% PI Low	Data Mean	95% PI High
Droplet size	13.9909	13.9909	0.771359	2.59257	7.64711	14.4875	20.3347
PDI	0.15236	0.15236	0.0174139	0.058529	0.0091447	0.1815	0.295575

3.2. Characterization of the Optimal VCZ-Loaded Nanoemulsion and Stability Studies

Optimal VCZ-loaded nanoemulsion was composed of 3.345% corn oil, 3.345% PSEO, 3.238% Span® 80, 16.188% Kolliphore® EL, 3.885% Transcutol® HP, 69% water, and 1% VCZ. It was subject to a physicochemical characterization (macroscopic aspect, droplet size, PDI, zeta potential percentage of transmittance, and pH) and different thermodynamic stability tests (centrifugation, freeze–thaw cycles, and heating–cooling cycles). The results of these studies are summarized in Table 4.

Table 4. Physicochemical characterization and stability tests of the optimal VCZ-loaded nanoemulsion.

	Parameters	Results
Physicochemical characterization	Macroscopic aspect	Translucent with a typical blue-shining appearance
	Droplet size (nm)	19.067 nm ± 0.138 nm
	PDI	0.147 ± 0.010
	Zeta potential (mV)	−17.433 ± 1.457 mV
	Percentage of transmittance (%)	95.489% ± 0.139%
	pH	5.64 ± 0.03
Stability studies	Centrifugation	Stable
	Freeze–thaw cycles	Stable
	Heating–cooling cycles	Stable

Macroscopically, the optimized formulation appeared translucent with a typical blue-shining appearance (Figure S5—Supplementary Materials). It presented a droplet size of 19.067 nm ± 0.138 nm (<100 nm), a PDI less than 0.3 (0.147 ± 0.010), a zeta potential of −17.433 ± 1.457 mV, a percentage of transmittance of 95.489% ± 0.139% (≈100%), and a pH value of 5.64 ± 0.03.

Moreover, no sign of macroscopic instability (phase separation, creaming, cracking, etc.) or drug precipitation occurred after the different stability tests, which highlights its great physical stability.

3.3. In Vitro Cytotoxicity Assay

To assess the effect of the VCZ free drug (VCZ), unload nanoemulsion (NE-Blank), and VCZ-loaded nanoemulsion (NE-VCZ) on HacaT cell viability, a colorimetric MTT assay was performed. The findings from Figure 3 demonstrated that both NE-VCZ and NE-Blank formulations showed cell toxicity at concentrations above 12.5 µg/mL, meanwhile VCZ was safe up to 50 µg/mL.

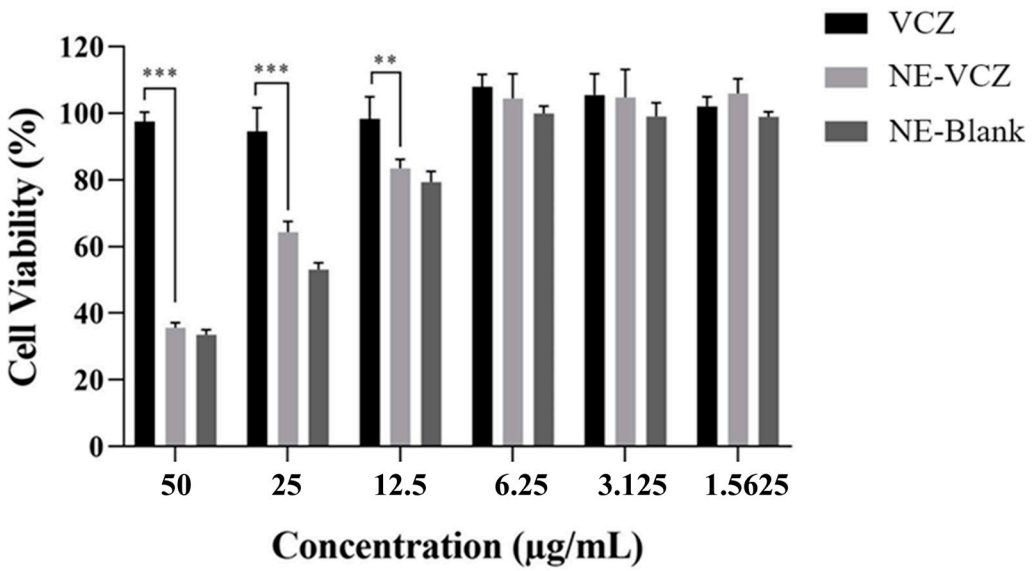

Figure 3. Cell viability results of HacaT cells after incubation with different samples: voriconazole (VCZ), VCZ-loaded nanoemulsion (NE-VCZ), and unloaded nanoemulsion (NE-Blank). Data are expressed as mean ± SD (n = 4). Significant statistical differences: ** $p < 0.01$ and *** $p < 0.001$.

3.4. In Vitro Permeability Studies

Figure 4 represents the diffusion profiles of the VCZ free drug (suspension) *versus* the optimal nanoemulsion across the dialysis membrane using the Franz diffusion cell system.

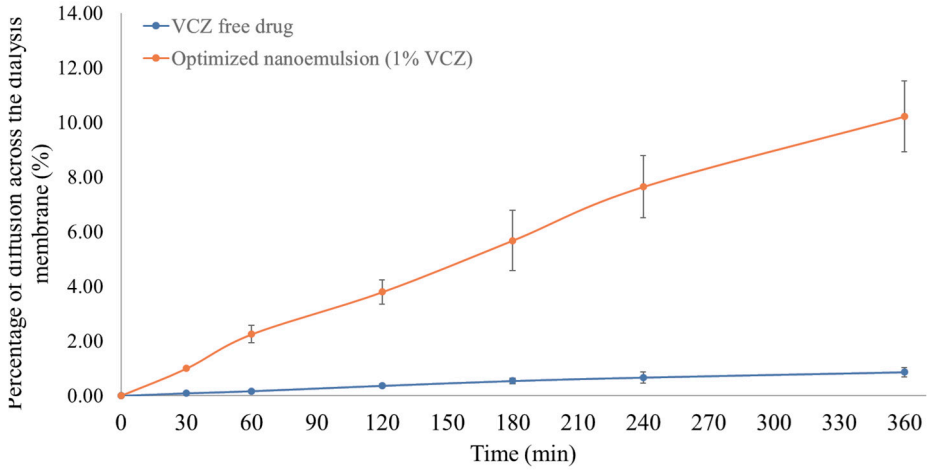

Figure 4. In vitro diffusion profiles of voriconazole free drug (—●—) and optimized nanoemulsion (—●—) using dialysis membrane as a model.

As reported in the graph, the VCZ suspension exhibited a lower diffusion profile in comparison with the optimized formulation. As an example, at 60 min, 0.171% ± 0.041% and 2.246% ± 0.316% of drug diffused from donor to receptor compartment for the VCZ free drug and the VCZ-loaded nanoemulsion, respectively. At the end of the experiment (360 min), the diffused fraction of VCZ was 0.857% ± 0.167% and 10.218% ± 1.288% for the VCZ suspension and the optimized formulation, respectively.

The comparison of the diffusion profiles of the two samples (free drug versus nanoemulsion) was made using the similarity test, which consisted in the determination of the difference factor (f_1) and the similarity factor (f_2). The calculated values of f_1 and f_2 were 1037.76% (>15%) and 62.74% (>50%), respectively, indicating the non-similarity of the two profiles.

Apparent permeability coefficients P_{app} (cm/s) are depicted in Figure 5. Results were expressed, in cm/s, as mean ± standard error of three experiments (n = 3).

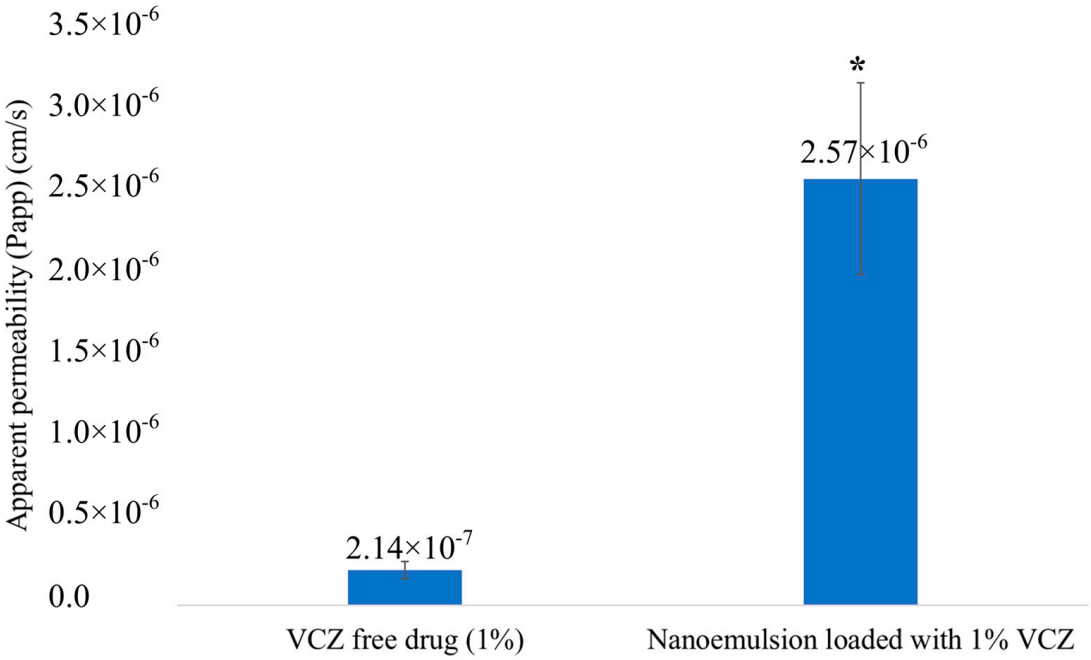

Figure 5. Apparent permeability coefficient (Papp) across the dialysis membrane for VCZ pure drug and VCZ optimal nanoemulsion. Data are presented as mean ± standard error of three determinations (n = 3). * Significant at the level of 95% ($p < 0.05$).

The apparent permeability values were 2.142 × 10^{-7} cm/s ± 0.522 × 10^{-7} cm/s and 2.573 × 10^{-6} cm/s ± 0.577 × 10^{-6} cm/s for VCZ suspension and VCZ-loaded optimal nanoemulsion, respectively. These results indicate that, compared to the VCZ free drug, a significant improvement in P_{app} occurred in the case of the optimized formulation ($p \leq 0.05$).

3.5. In Vitro Antifungal Activity

The results of the disk diffusion assay for VCZ-SUSP, PSEO, NE-Blank, and NE-VCZ are depicted in Figure 6. The inhibition zone diameters (IZDs) were 61.66 mm ± 1.52 mm, 48.33 mm ± 1.52 mm, and 80.33 mm ± 4.61 mm for VCZ-SUSP, PSEO, and NE-VCZ, respectively, whereas NE-Blank exhibited no activity (IZD = 0 mm). According to IZD results, the optimized nanoemulsion showed noticeably better antifungal activity against *Microsporum canis* in comparison to VCZ or PSEO. This finding suggests that the nanoemulsion formulation improved voriconazole distribution and effectiveness and highlights the synergetic effect of PSEO and VCZ since their association resulted in a better antifungal activity than that of each component used alone.

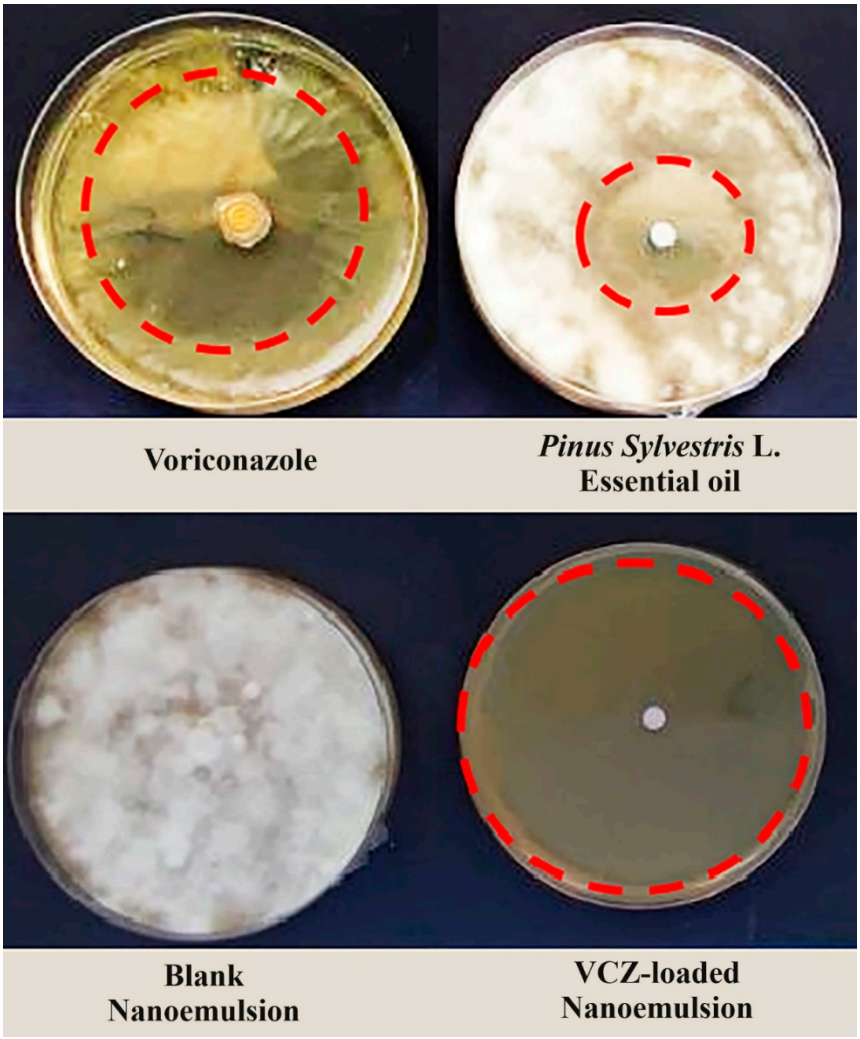

Figure 6. Disk agar diffusion assay of voriconazole, *Pinus sylvestris* L. essential oil, blank nanoemulsion (unloaded), and VCZ-loaded nanoemulsion against *Microsporum canis* clinical strain.

4. Discussion

This study aimed to explore the antifungal potential of an innovative formulation (o/w nanoemulsion) containing VCZ, a triazole antifungal agent with good effectiveness against a variety of fungi, including Candida species and dermatophytes [6,38], associated with *Pinus sylvestris* L. essential oil (PSEO).

In order to delimit the nanoemulsion region and to find the concentration range of each excipient used for the formulation, various pseudo-ternary phase diagrams were constructed using the water titration method (a low-energy method). Corn oil (density: 0.915–0.918 g/cm^3; viscosity: 37–39 cP) was selected as solvent [39]. It is a vegetable oil rich in linoleic (C18:2; 34.0–65.6%), oleic (C18:1, 20.0–42.2%), and palmitic (C16:0; 8.6–16.5%) acids [40]. Transcutol® HP was used as cosolvent. It is a nontoxic and good solubilizing excipient for drugs and a skin penetration enhancer [41]. Kolliphore® EL, a non-ionic hydrophilic surfactant with a high HLB value of 12–14, was chosen as surfactant considering the ability of such excipients to facilitate the formation of droplets with a small size by low-energy methods [42,43]. Finally, Span® 80 (HLB value of 4.3) was used as cosurfactant. Generally, the use of a single surfactant is not efficient to lower enough the surface tension at the oil/water interface to obtain droplets with sizes in the nanoscale range. A cosurfactant will permit to obtain a more fluid and flexible interfacial film by altering its molecular geometry, allowing for reaching a smaller droplet size [44,45].

Three pseudo-ternary phase diagrams were established by varying the surfactant/cosurfactant (Smix) to cosolvent (CoS) weight ratio from 1:1 (*wt*/*wt*) to 5:1 (*wt*/*wt*). An enlargement of the nanoemulsion region was noticed as the amount of Smix increased, which may be explained by the additional lowering in surface tension and a greater increase in the fluidity of the interfacial film [46]. Consequently, the pseudo-ternary diagram obtained with a Smix/CoS ratio of 5:1 (*wt*/*wt*) was retained for the optimization step.

D-optimal mixture design was used to determine the optimal nanoemulsion composition by studying the effect of three variables (percentage of Smix/CoS, percentage of water, and percentage of oil mixture) on two responses, which were droplet size and PDI.

According to low and high predefined levels for each component, a new experimental region representing a subregion of the nanoemulsion area was generated and explored. Sixteen formulations were proposed by the design of experiment software. They were prepared and assessed for their droplet size and PDI. Results of both responses were analyzed and fitted to numerous mathematical models proposed by Design-Expert® software. The statistical analysis allowed for identifying the cubic model as the best-fitting mathematical model for the two studied responses since the latter presented (1) significant sequential *p*-values ($p < 0.05$); (2) non-significant lack of fit *p*-values ($p > 0.05$); (3) the lowest standard deviation values; (4) the highest squared correlation coefficients (R^2); (5) differences between the adjusted R^2 and the predicted R^2 less than 0.2; and (6) the lowest predicted residual sum of squares (PRESSs) [47]. The postulated mathematical models were represented by polynomial equations whose coefficients were used to understand how the three variables (Smix/CoS, water, and oil mixture) interact with each other and how that affects the droplet size and the PDI. A high positive coefficient value of a variable signifies a positive effect on the studied response, while a high negative coefficient value suggests the opposite effect [47]. The effect of the variable on droplet size and PDI were also investigated using the Cox response trace plot (graphical analysis) for a better explanation. The latter shows the influence of each constituent of the mixture on the studied response in relation to a reference formulation (defined by the center point). The predicted response is traced by varying the percentage of the studied constituent from the center point while the other components are held at a fixed level. A curve nearly horizontal indicates that the variable has a slight effect on the response, while a pronounced deviation of the curve from the *x*-axis signifies that the response is sensitive to the change in the components' proportion [34]. According to our findings, the amount of Smix/CoS or oil mixture significantly affects both responses. When the proportion of Smix/CoS increased, both droplet size and PDI decreased (negative effect), whereas an increase in the oil mixture led to an increase in the two responses (positive effect). These results are in good accordance with previously published works where the authors reported similar observations [47–50]. A desirability function was used to optimize both droplet size and PDI simultaneously [47]. Its aim was to find the proportion of each component (Smix/CoS, water, and oil mixture) that ensures compliance with the criteria of the two studied responses, with a desirability value closest to 1 (the closer the obtained value of the desirability is to 1, the more closely the proposed solution matches the desired optimal formulation [51]). The target of the optimization step was to minimize both responses in order to improve the stability of the formulation and to increase drug permeation through the nail barrier while maximizing the amount of oil mixture (to solubilize the greatest amount of antifungal agent) as well as the proportion of Smix/CoS.

Optimized VCZ-loaded nanoemulsion was assessed for macroscopic aspect, droplet size, PDI, zeta potential, pH, percentage of transmittance, and physical stability. Macroscopically, it was translucent with a bluish aspect, suggesting the existence of the dispersed phase on a nanoscale level [52]. It showed a small droplet size that was in the nanometer range (20–200 nm) [53] and a polydispersity index (PDI) less than 0.3, indicating a narrow size distribution of the droplets, which reflects the homogeneity of the dispersed phase [34]. The zeta potential value was higher than |15| mV, indicating its good stability [54]. Its pH

value was within the physiological range of skin (pH 4.0–6.0) [55]. Finally, its percentage of transmittance was found to be close to 100%, reflecting its high transparency.

Regarding the in vitro cytotoxicity study, different concentrations of VCZ, as well as unloaded nanoemulsion (NE-Blank) and VCZ-loaded nanoemulsion (NE-VCZ) formulations, were tested using HacaT cells to find out from which concentration a potential cytotoxicity could appear. According to the cell viability evaluation, we were able to confirm that VCZ at the tested concentrations was not toxic to the cells. These results are in good accordance with a study conducted by Cheaburu-Yilmaz et al., where they showed that VCZ had no cytotoxic effect on rat embryonic fibroblast cells (NIH-3T3) at 100 µg/mL concentration [56]. Concerning the formulation of the nanoemulsion, one of the criteria taken into consideration for the selection of the surfactant (Kolliphor® EL), the cosurfactant (Span® 80), and the cosolvent (Transcutol® HP) was their low toxicity toward skin tissues. In fact, these components are widely used to formulate nanosystems (nanoemulsions, microemulsions, self-emulsifying drug delivery systems, etc.) for different routes (ocular, topical, oral, etc.) because they are less toxic in comparison to other excipients such as ionic surfactants. However, certain components, such as nanoemulsion stabilizers or surfactants, are well recognized to cause toxicity in cultured cells due to their solubilizing properties [57,58], despite being labeled as biocompatible. The in vitro cytotoxicity assay showed toxicity concentration-dependence, which occurred at high concentrations (above 12,5 µg/mL) of NE-Blank and NE-VCZ with a decrease in cell viability. These findings are in accordance with data reported previously. According to the literature, the exposure of the cellular membrane to non-ionic surfactants such as Polysorbate 80 and Kolliphor® EL promotes a decrease in their glutathione levels, leading to an increase in hydrogen peroxide cytotoxicity, which causes oxidative stress [59–61]. A study conducted by Zanatta et al. demonstrated that Span® 80 had a concentration-dependent toxicity on both skin cell lines (3T3-L1 and HaCaT cells) [62]. Bunchongprasert et al. highlighted the fact that the use of Kolliphor® EL in nanosystem formulation caused cytotoxicity that was both time- and concentration-dependent [63]. Another study conducted by Ruhl et al. revealed that Kolliphor® EL had no cytotoxic effect on preadipocytes at lower concentrations; however, as the concentration of the surfactant increased, the viable cell number decreased over time [64]. Finally, a recent report demonstrated that the microemulsion encapsulating the Benjakul (BJK) extract used as an active ingredient showed cell toxicity at concentrations above 20 µg/mL, while BJK was safe up to 50 µg/mL [65].

In vitro permeation studies of a VCZ free drug (suspensions) versus an optimized VCZ-loaded nanoemulsion were performed using a Franz diffusion cell as a system and dialysis membrane as a diffusion model. The diffusion profiles (drug diffusion percentage over time) of both preparations were compared by applying the similarity test (f_1 and f_2). The obtained results showed a significant difference between the two diffusion curves. The VCZ nanoemulsion exhibited a higher diffusion profile in comparison with the VCZ free drug. Same findings were noticed for the coefficient of permeability (Papp), with an increase of 12-fold for the optimized nanoemulsion when compared to the VCZ suspension.

VCZ is a class II BCS, which means low solubility and high permeability [66]. Poor aqueous solubility is a limiting factor for drug absorption. The use of an innovative drug delivery system, viz., nanoemulsion, improved VCZ permeation. This enhancement could be attributed to (1) its high solubilization capacity of the VCZ and (2) to the nanoscale size of the dispersed phase, which leads to a large interfacial area in contact with the dialysis membrane, enabling efficient drug transport [67,68].

The antifungal effectiveness of the VCZ free drug, *Pinus sylvestris* L. essential oil, unloaded nanoemulsion (NE-Blank), and VCZ-loaded nanoemulsion (NE-VCZ) was tested on a dermatophyte, *Microsporum canis*, isolated from a nail with onychomycosis diagnosis (Laboratory of Parasitology and Mycology of the Fattouma Bourguiba University Hospital in Monastir-Tunisia), using a disk-agar diffusion assay.

VCZ demonstrated good antifungal efficiency. Indeed, a clear inhibition zone was observed with a diameter of inhibition of 61.66 mm ± 1.52 mm. This finding is in good

agreement with the literature. In a previous publication, Nweze EI et al. studied the in vitro antifungal activities of eight antifungal agents, including voriconazole, against 37 strains of dermatophytes using an agar-based disk diffusion assay. The authors found inhibition zone diameter values of 38.00 mm ± 2.36 mm, 33.38 mm ± 3.05 mm, 55.50 mm ± 5.43 mm, and 66.67 mm ± 6.83 mm for VCZ (1 µg/disk) against *Trichophyton tonsurans*, *Trichophyton mentagrophytes*, *Microsporum canis*, and *Epidermophyton floccosum* strains, respectively [37]. The VCZ antifungal mechanism involves the decrease in the synthesis of ergosterol, an essential component of fungal cell membranes, by inhibiting 14-alpha-lanosterol demethylation, which leads to a disruption of cell membrane integrity [69].

PSEO showed a good but less strong antimycotic effect than VCZ with an inhibition zone of 48.33 mm w ± 1.52 mm. Several studies have investigated and highlighted the antifungal activity of PSEO [23,26,70,71]. Its efficacy could be attributed to the complex composition of this essential oil. A GC/MS analysis was carried out to identify the chemical composition of PSEO utilized in our study (unshown data). The major constituents found included α-Pinene (40.26%), β-Pinene (20.21%), β-Myrcene (2.13%), δ-3-Carene (16.46%), p-Cymene (1.58%), and Limonene (9.67%) as monoterpene hydrocarbons; Bornyl Acetate (1.83%) as oxygenated monoterpenes; and β-Caryophyllene (1.82%) as sesquiterpene hydrocarbons. These chemical constituents may act by destabilizing the cell membrane integrity and damaging mitochondria and DNA of the fungus [72–75]. Indeed, α-pinene and limonene cause impairment to the fungal cell membrane, increasing its permeability, as well as efficient ions and intracellular macromolecular substances (such as proteins) leakage, resulting in cell death. They also affect cell growth and morphology. Moreover, limonene causes failure of ion transfer and generation of ATP. α-pinene acts by binding ergosterol and by inhibiting phospholipase and esterase enzyme activities [76–78]. β-pinene disrupts cell membrane integrity by inhibiting the function of fungal mitochondria [79]. Bornyl acetate impacts cell growth and disrupts membrane structure by affecting enzyme activity, as well as penetrating the lipids of both mitochondrial and cytoplasmic membranes [78]. Myrcene affects cell integrity and morphology and causes genetic alterations [80]. Finally, caryophyllene may act by interacting with the structure of the fungal membrane, which influences the development of its mycelium. It induces damage to the cell wall, affecting the polar group (phosphate group), leading to a breaking down of the phospholipid molecule into glycerol, carboxylic acid, and phosphoric acid. As a result, phospholipids are unable to preserve the integrity of the cell membrane, resulting in cell death [81].

The placebo nanoemulsion (unloaded formulation) did not exhibit any fungicidal activity, unlike the optimized nanoemulsion, which exhibited the strongest antimycotic activity among the four tested samples with an inhibition zone of 80.33 mm ± 4.61 mm. This observation highlights the synergetic effect between PSEO and VCZ. This combination may improve the antifungal efficacy through synergistic mechanisms, including (1) increased cell membrane permeability, which allows the antifungal agent to penetrate the fungal cell at a more effective level and to reach its target sites; (2) inhibition of efflux pumps to overcome resistance to antifungal molecules; and (3) enhanced ergosterol inhibition [73,75,82].

5. Conclusions

The present study aimed to assess the antimycotic efficacy of a topical o/w nanoemulsion formulation containing voriconazole (VCZ) combined with *Pinus sylvestris* L. essential oil (PSEO). The formulation of the innovative form was realized in two steps: the use of the pseudo-ternary phase diagram to delimit the nanoemulsion region, followed by the application of the D-optimal mixture design for the optimization. The optimized nanoemulsion exhibited suitable physicochemical characteristics (droplet size, PDI, percentage of transmittance, zeta potential, and pH) for topical drug delivery and good physical stability (absence of any sign of macroscopic instability). In addition, it showed significantly better in vitro permeation in comparison with the VCZ free drug. Finally, in vitro antifungal activity has proven the effectiveness of this novel formulation against the *Microsporum canis* clinical strain in comparison with VCZ and PSEO used alone, highlighting their synergetic

effect. Further ex vivo and clinical investigations are needed to support these promising results in the treatment of onychomycosis.

Supplementary Materials: The following supporting information can be downloaded at: https://www.mdpi.com/article/10.3390/colloids8050056/s1, Figure S1: Experimental points generated by the Design of Experiment software in the nanoemulsion region; Figure S2: Franz cell diffusion system: (1) Donor chamber; (2) Receptor chamber; (3) Franz cell clamp; (4) Dialysis membrane; (5) Stir bar; (6) Sampling port; Figure S3: Franz cell assembly for in vitro diffusion study of voriconazole: (1) Franz cell diffusion system; (2) Water bath; (3) Magnetic stirrer; Figure S4: Macroscopic aspect of the sixteen runs generated by Design-Expert® Software; Figure S5: Macroscopic aspect of the optimal VCZ-loaded nanoemulsion with a translucent appearance and a bluish brightness; Table S1: Summary of the results of statistical analyses for response Y1 (Droplet size)—Design-Expert® software; Table S2: Summary of the results of statistical analyses for response Y2 (PDI)—Design-Expert® software.

Author Contributions: Conceptualization, M.A.L. and S.H.M.A.-S.; methodology, S.H.M.A.-S., O.B.H.A., M.A.L., S.S., H.B. and L.C.-G.; software, O.B.H.A. and M.A.L.; validation, M.A.L., S.S., H.B. and L.C.-G.; formal analysis, S.H.M.A.-S., R.C.-B., T.K. and M.R.S.; investigation, S.H.M.A.-S.; resources, S.H.M.A.-S.; data curation, S.H.M.A.-S., R.C.-B. and T.K.; writing—original draft preparation, S.H.M.A.-S., R.C.-B., T.K. and M.R.S.; writing—review and editing, M.A.L., S.S., H.B. and L.C.-G.; visualization, S.H.M.A.-S. and M.A.L.; supervision, M.A.L.; project administration, S.H.M.A.-S. and M.A.L. All authors have read and agreed to the published version of the manuscript.

Funding: This research received no external funding.

Data Availability Statement: All the data in this study are included in the manuscript and Supplementary Materials. Enquiries may be made to the corresponding authors.

Conflicts of Interest: The authors declare no conflicts of interest.

References

1. Ojha, A.K.; Albert, V.; Sharma, S.; Hallur, V.; Singh, G.; Pamidimukkala, U.; Singh, K.J.; Kaur, H.; Karuna, T.; Savio, J.; et al. Pan-Indian Clinical Registry of Invasive Fungal Infections Among Patients in the Intensive Care Unit: Protocol for a Multicentric Prospective Study. *JMIR Res. Protoc.* **2024**, *13*, e54672. [CrossRef]
2. Chanyachailert, P.; Leeyaphan, C.; Bunyaratavej, S. Cutaneous fungal infections caused by dermatophytes and non-dermatophytes: An Updated Comprehensive Review of Epidemiology, Clinical presentations, and diagnostic testing. *J. Fungi* **2023**, *9*, 669. [CrossRef]
3. Maskan Bermudez, N.; Rodríguez-Tamez, G.; Perez, S.; Tosti, A. Onychomycosis: Old and New. *J. Fungi* **2023**, *9*, 559. [CrossRef]
4. Lipner, S.R.; Scher, R.K. Onychomycosis: Clinical overview and diagnosis. *J. Am. Acad. Dermatol.* **2019**, *80*, 835–851. [CrossRef]
5. Sigurgeirsson, B.; Baran, R. The prevalence of onychomycosis in the global population–a literature study. *J. Eur. Acad. Dermatol. Venereol.* **2014**, *28*, 1480–1491. [CrossRef]
6. Carrillo-Muñoz, A.J.; Giusiano, G.; Guarro, J.; Quindós, G.; Guardia, C.; del Valle, O.; Rodríguez, V.; Estivill, D.; Cárdenes, C.D. In vitro activity of voriconazole against dermatophytes, Scopulariopsis brevicaulis and other opportunistic fungi as agents of onychomycosis. *Int. J. Antimicrob. Agents* **2007**, *30*, 157–161. [CrossRef]
7. Shirwaikar, A.; Thomas, T.; Shirwaikar, A.; Lobo, R.; Prabhu, K. Treatment of onychomycosis: An update. *Indian. J. Pharm. Sci.* **2008**, *70*, 710–714. [CrossRef]
8. Gupta, A.K.; Talukder, M.; Venkataraman, M. Review of the alternative therapies for onychomycosis and superficial fungal infections: Posaconazole, fosravuconazole, voriconazole, oteseconazole. *Int. J. Dermatol.* **2022**, *61*, 1431–1441. [CrossRef]
9. Nofal, A.; Fawzy, M.M.; El-Hawary, E.E. Successful treatment of resistant onychomycosis with voriconazole in a liver transplant patient. *Dermatol. Ther.* **2020**, *33*, e14014. [CrossRef]
10. Axler, E.; Lipner, S.R. Antifungal Selection for the Treatment of Onychomycosis: Patient Considerations and Outcomes. *Infect. Drug Resist.* **2024**, *17*, 819–843. [CrossRef]
11. de Almeida Campos, L.; Fin, M.T.; Santos, K.S.; de Lima Gualque, M.W.; Freire Cabral, A.K.L.; Khalil, N.M.; Fusco-Almeida, A.M.; Mainardes, R.M.; Mendes-Giannini, M.J.S. Nanotechnology-Based Approaches for Voriconazole Delivery Applied to Invasive Fungal Infections. *Pharmaceutics* **2023**, *15*, 266. [CrossRef]
12. Scott, L.J.; Simpson, D. Voriconazole: A review of its use in the management of invasive fungal infections. *Drugs* **2007**, *67*, 269–298. [CrossRef]
13. Donnelly, J.P.; De Pauw, B.E. Voriconazole-a new therapeutic agent with an extended spectrum of antifungal activity. *Clin. Microbiol. Infect.* **2004**, *10*, 107–117. [CrossRef]
14. Maschmeyer, G.; Haas, A. Voriconazole: A broad spectrum triazole for the treatment of serious and invasive fungal infections. *Future Microbiol.* **2006**, *1*, 365–385. [CrossRef]

15. Akkuş, İ.; Kaçmaz, B. Antifungal drugs. *J. Curr. Hematol. Oncol. Res.* **2023**, *1*, 41–46. [CrossRef]
16. Poojary, S.A. Topical antifungals: A review and their role in current management of dermatophytoses. *Clin. Dermatol. Rev.* **2017**, *1* (Suppl. 1), S24–S29. [CrossRef]
17. Rathi, A.R.; Popat, R.R.; Adhao, V.S.; Shrikhande, V.N. Nail drug delivery system a review. *Int J Pharm Chem Anal* **2020**, *7*, 9–21.
18. Gupta, A.K.; Polla Ravi, S.; Choi, S.Y.; Konda, A.; Cooper, E.A. Strategies for the enhancement of nail plate permeation of drugs to treat onychomycosis. *J. Eur. Acad. Dermatol. Venereol.* **2023**, *37*, 243–255. [CrossRef]
19. Lang, G.; Buchbauer, G. A review on recent research results (2008–2010) on essential oils as antimicrobials and antifungals. A review. *Flavour. Fragr. J.* **2012**, *27*, 13–39. [CrossRef]
20. Cannas, S.; Usai, D.; Tardugno, R.; Benvenuti, S.; Pellati, F.; Zanetti, S.; Molicotti, P. Chemical composition, cytotoxicity, antimicrobial and antifungal activity of several essential oils. *Nat. Prod. Res.* **2016**, *30*, 332–339. [CrossRef]
21. Vaou, N.; Stavropoulou, E.; Voidarou, C.; Tsigalou, C.; Bezirtzoglou, E. Towards Advances in Medicinal Plant Antimicrobial Activity: A Review Study on Challenges and Future Perspectives. *Microorganisms* **2021**, *9*, 2041. [CrossRef]
22. Khan, M.S.A.; Malik, A.; Ahmad, I. Anti-candidal activity of essential oils alone and in combination with amphotericin B or fluconazole against multi-drug resistant isolates of Candida albicans. *Med. Mycol.* **2012**, *50*, 33–42. [CrossRef]
23. Scalas, D.; Mandras, N.; Roana, J.; Tardugno, R.; Cuffini, A.M.; Ghisetti, V.; Benvenuti, S.; Tullio, V. Use of *Pinus sylvestris* L. (Pinaceae), *Origanum vulgare* L. (Lamiaceae), and *Thymus vulgaris* L. (Lamiaceae) essential oils and their main components to enhance itraconazole activity against azole susceptible/not-susceptible Cryptococcus neoformans strains. *BMC Complement. Altern. Med.* **2018**, *18*, 1–13. [CrossRef]
24. Wróblewska, M.; Szymańska, E.; Winnicka, K. The influence of tea tree oil on antifungal activity and pharmaceutical characteristics of Pluronic® F-127 gel formulations with ketoconazole. *Int. J. Mol. Sci.* **2021**, *22*, 11326. [CrossRef]
25. Roana, J.; Mandras, N.; Scalas, D.; Campagna, P.; Tullio, V. Antifungal activity of Melaleuca alternifolia essential oil (TTO) and its synergy with itraconazole or ketoconazole against Trichophyton rubrum. *Molecules* **2021**, *26*, 461. [CrossRef]
26. Motiejūnaitė, O.; Dalia Pečiulytė, D. Fungicidal properties of *Pinus sylvestris* L. for improvement of air quality. *Medicina* **2004**, *8*, 787–794.
27. Rózalska, B.; Sadowska, B.; Wieckowska-Szakiel, M.; Budzyńska, A. [The synergism of antifungals and essential oils against Candida spp. evaluated by a modified gradient-diffusion method], Synergizm leków przeciwgrzybiczych i olejków eterycznych wobec *Candida* sp., oceniany zmodyfikowana metoda gradientowo-dyfuzyjna. *Med. Dosw. Mikrobiol.* **2011**, *63*, 163–169.
28. Sharifzadeh, A.; Shokri, H.; Abbaszadeh, S. Interaction of carvacrol and voriconazole against drug-resistant Candida strains isolated from patients with candidiasis. *J. Mycol. Med.* **2019**, *29*, 44–48. [CrossRef]
29. Chen, L.; Tan, F.; Wang, J.; Liu, F. Assessment of the percutaneous penetration of indomethacin from soybean oil microemulsion: Effects of the HLB value of mixed surfactants. *Pharmazie* **2012**, *67*, 31–36.
30. Thongchai, W.; Liawruangrath, B. Development of HPLC analysis for the determination of retinol and alpha tocopherol in corn oil nanoemulsion lotion. *Int. Food Res. J.* **2016**, *23*, 1367–1371.
31. Ryu, K.-A.; Park, P.J.; Kim, S.-B.; Bin, B.-H.; Jang, D.-J.; Kim, S.T. Topical delivery of coenzyme Q10-loaded microemulsion for skin regeneration. *Pharmaceutics* **2020**, *12*, 332. [CrossRef]
32. Orchard, A.; van Vuuren, S.F.; Viljoen, A.M. Commercial essential oil combinations against topical fungal pathogens. *Nat. Prod. Commun.* **2019**, *14*, 1934578X1901400139. [CrossRef]
33. Felšöciová, S.; Vukovic, N.; Jeżowski, P.; Kačániová, M. Antifungal activity of selected volatile essential oils against *Penicillium* sp. *Open Life Sci.* **2020**, *15*, 511–521. [CrossRef]
34. Rasoanirina, B.N.V.; Lassoued, M.A.; Kamoun, A.; Bahloul, B.; Miladi, K.; Sfar, S. Voriconazole-loaded self-nanoemulsifying drug delivery system (SNEDDS) to improve transcorneal permeability. *Pharm. Dev. Technol.* **2020**, *25*, 694–703. [CrossRef]
35. Lassoued, M.A.; Sfar, S.; Bouraoui, A.; Khemiss, F. Absorption enhancement studies of clopidogrel hydrogen sulphate in rat everted gut sacs. *J. Pharm. Pharmacol.* **2012**, *64*, 541–552. [CrossRef]
36. Lassoued, M.A.; Khemiss, F.; Sfar, S. Comparative study of two in vitro methods for assessing drug absorption: Sartorius SM 16750 apparatus versus everted gut sac. *J. Pharm. Pharm. Sci.* **2011**, *14*, 117–127. [CrossRef]
37. Nweze, E.I.; Mukherjee, P.; Ghannoum, M. Agar-based disk diffusion assay for susceptibility testing of dermatophytes. *J. Clin. Microbiol.* **2010**, *48*, 3750–3752. [CrossRef]
38. Uzun, O.; Arikan, S.; Kocagöz, S.; Sancak, B.; Unal, S. Susceptibility testing of voriconazole, fluconazole, itraconazole and amphotericin B against yeast isolates in a Turkish University Hospital and effect of time of reading. *Diagn. Microbiol. Infect. Dis.* **2000**, *38*, 101–107. [CrossRef]
39. Rowe, R.C.; Sheskey, P.; Quinn, M. *Handbook of Pharmaceutical Excipients*, 6th ed.; Pharmaceutical Press and American Pharmacists Association: Grayslake, IL, USA, 2009; pp. 199–200.
40. Barrera-Arellano, D.; Badan-Ribeiro, A.P.; Serna-Saldivar, S.O. Corn oil: Composition, processing, and utilization. In *Corn: Chemistry and Technology*, 3rd ed.; Serna-Saldivar, S.O., Ed.; Woodhead Publishing and AACC International Press: Cambridge, UK, 2019; pp. 593–613.
41. Osborne, D.W.; Musakhanian, J. Skin penetration and permeation properties of Transcutol®-neat or diluted mixtures. *Aaps Pharmscitech* **2018**, *19*, 3512–3533. [CrossRef]
42. Séguy, L.; Groo, A.-C.; Goux, D.; Hennequin, D.; Malzert-Fréon, A. Design of non-haemolytic nanoemulsions for intravenous administration of hydrophobic APIs. *Pharmaceutics* **2020**, *12*, 1141. [CrossRef]

43. Smejkal, G.; Gross, V.; Lazarev, A. Theoretical and Experimental Determinations of the Hydrophilic–Lipophilic Balance (HLB) of Representative Oils and Lecithins. *Colloids Interfaces* **2024**, *8*, 21. [CrossRef]
44. Azeem, A.; Rizwan, M.; Ahmad, F.J.; Iqbal, Z.; Khar, R.K.; Aqil, M.; Talegaonkar, S. Nanoemulsion components screening and selection: A technical note. *AAPS PharmSciTech* **2009**, *10*, 69–76. [CrossRef]
45. Wooster, T.J.; Labbett, D.; Sanguansri, P.; Andrews, H. Impact of microemulsion inspired approaches on the formation and destabilisation mechanisms of triglyceride nanoemulsions. *Soft Matter* **2016**, *12*, 1425–1435. [CrossRef]
46. Shakeel, F.; Salem-Bekhit, M.M.; Haq, N.; Alshehri, S. Nanoemulsification improves the pharmaceutical properties and bioactivities of niaouli essential oil (*Melaleuca quinquenervia* L.). *Molecules* **2021**, *26*, 4750. [CrossRef]
47. Ben Hadj Ayed, O.; Lassoued, M.A.; Bahloul, B.; Sfar, S. Self-emulsifying drug delivery system for improved dissolution and oral absorption of quetiapine fumarate: Investigation of drug release mechanism and in-vitro intestinal permeability. *Iran. J. Pharm. Res.* **2021**, *20*, 381.
48. Pestana, K.; Formariz, T.; Franzini, C.; Sarmento, V.; Chiavacci, L.; Scarpa, M.; Egito, E.; Oliveira, A.G.d. Oil-in-water lecithin-based microemulsions as a potential delivery system for amphotericin B. *Colloids Surf. B Biointerfaces* **2008**, *66*, 253–259. [CrossRef]
49. Sakeena, M.H.; Elrashid, S.M.; Munavvar, A.S.; Azmin, M.N. Effects of oil and drug concentrations on droplets size of palm oil esters (POEs) nanoemulsion. *J. Oleo Sci.* **2011**, *60*, 155–158. [CrossRef]
50. Sarheed, O.; Dibi, M.; Ramesh, K.V. Studies on the effect of oil and surfactant on the formation of alginate-based O/W lidocaine nanocarriers using nanoemulsion template. *Pharmaceutics* **2020**, *12*, 1223. [CrossRef]
51. Iskandar, B.; Mei, H.-C.; Liu, T.-W.; Lin, H.-M.; Lee, C.-K. Evaluating the effects of surfactant types on the properties and stability of oil-in-water Rhodiola rosea nanoemulsion. *Colloids Surf. B Biointerfaces* **2024**, *234*, 113692. [CrossRef]
52. Silva, D.; Sarruf, F.; Oliveira, L.; Arêas, E.; Kaneko, T.; Consiglieri, V.; Velasco, M.; Baby, A. Influence of particle size on appearance and *in vitro* efficacy of sunscreens. *Braz. J. Pharm. Sci.* **2013**, *49*, 251–261. [CrossRef]
53. Jaiswal, M.; Dudhe, R.; Sharma, P. Nanoemulsion: An advanced mode of drug delivery system. *3 Biotech* **2015**, *5*, 123–127. [CrossRef]
54. Bhattacharjee, S. DLS and zeta potential–what they are and what they are not? *J. Control Release* **2016**, *235*, 337–351. [CrossRef]
55. Lukić, M.; Pantelić, I.; Savić, S.D. Towards optimal ph of the skin and topical formulations: From the current state of the art to tailored products. *Cosmetics* **2021**, *8*, 69. [CrossRef]
56. Cheaburu-Yilmaz, C.N.; Yilmaz, O.; Aydin Kose, F.; Bibire, N. Chitosan-graft-poly (N-isopropylacrylamide)/PVA cryogels as carriers for mucosal delivery of voriconazole. *Polymers* **2019**, *11*, 1432. [CrossRef]
57. Józsa, L.; Vasvári, G.; Sinka, D.; Nemes, D.; Ujhelyi, Z.; Vecsernyés, M.; Váradi, J.; Fenyvesi, F.; Lekli, I.; Gyöngyösi, A. Enhanced antioxidant and anti-inflammatory effects of self-nano and microemulsifying drug delivery systems containing curcumin. *Molecules* **2022**, *27*, 6652. [CrossRef]
58. Vater, C.; Adamovic, A.; Ruttensteiner, L.; Steiner, K.; Tajpara, P.; Klang, V.; Elbe-Bürger, A.; Wirth, M.; Valenta, C. Cytotoxicity of lecithin-based nanoemulsions on human skin cells and ex vivo skin permeation: Comparison to conventional surfactant types. *Int. J. Pharm.* **2019**, *566*, 383–390. [CrossRef]
59. Hirama, S.; Tatsuishi, T.; Iwase, K.; Nakao, H.; Umebayashi, C.; Nishizaki, Y.; Kobayashi, M.; Ishida, S.; Okano, Y.; Oyama, Y. Flow-cytometric analysis on adverse effects of polysorbate 80 in rat thymocytes. *Toxicology* **2004**, *199*, 137–143. [CrossRef]
60. Iwase, K.; Oyama, Y.; Tatsuishi, T.; Yamaguchi, J.Y.; Nishimura, Y.; Kanada, A.; Kobayashi, M.; Maemura, Y.; Ishida, S.; Okano, Y. Cremophor EL augments the cytotoxicity of hydrogen peroxide in lymphocytes dissociated from rat thymus glands. *Toxicol. Lett.* **2004**, *154*, 143–148. [CrossRef]
61. Tatsuishi, T.; Oyama, Y.; Iwase, K.; Yamaguchi, J.Y.; Kobayashi, M.; Nishimura, Y.; Kanada, A.; Hirama, S. Polysorbate 80 increases the susceptibility to oxidative stress in rat thymocytes. *Toxicology* **2005**, *207*, 7–14. [CrossRef]
62. Zanatta, C.F.; Ugartondo, V.; Mitjans, M.; Rocha-Filho, P.A.; Vinardell, M.P. Low cytotoxicity of creams and lotions formulated with Buriti oil (Mauritia flexuosa) assessed by the neutral red release test. *Food Chem. Toxicol.* **2008**, *46*, 2776–2781. [CrossRef]
63. Bunchongprasert, K.; Shao, J. Effect of fatty acid ester structure on cytotoxicity of self-emulsified nanoemulsion and transport of nanoemulsion droplets. *Colloids Surf. B Biointerfaces* **2020**, *194*, 111220. [CrossRef]
64. Ruhl, T.; Storti, G.; Pallua, N. Proliferation, Metabolic Activity, and Adipogenic Differentiation of Human Preadipocytes Exposed to 2 Surfactants In Vitro. *J. Pharm. Sci.* **2018**, *107*, 1408–1415. [CrossRef]
65. Kuropakornpong, P.; Itharat, A.; Ooraikul, B.; Loebenberg, R.; Davies, N.M. Development and optimization of Benjakul microemulsion formulations for enhancing topical anti-inflammatory effect and delivery. *Res. Pharm. Sci.* **2022**, *17*, 111–122. [CrossRef]
66. Sharma, A.; Katta, C.; Bahuguna, D.; Veerabomma, H.; Mourya, A.; Jyothi, V.; Dikundwar, A.; Singh, S.; Madan, J. Voriconazole-syringic acid co-crystals reduced voriconazole-induced hepatotoxicity: In vitro and in vivo studies. *J. Drug Deliv. Sci. Technol.* **2023**, *86*, 104685. [CrossRef]
67. Shaker, D.S.; Ishak, R.A.; Ghoneim, A.; Elhuoni, M.A. Nanoemulsion: A review on mechanisms for the transdermal delivery of hydrophobic and hydrophilic drugs. *Sci. Pharm.* **2019**, *87*, 17. [CrossRef]
68. Preeti; Sambhakar, S.; Malik, R.; Bhatia, S.; Al Harrasi, A.; Rani, C.; Saharan, R.; Kumar, S.; Geeta; Sehrawat, R. Nanoemulsion: An emerging novel technology for improving the bioavailability of drugs. *Scientifica* **2023**, *2023*, 6640103. [CrossRef]
69. Greer, N.D. Voriconazole: The Newest Triazole Antifungal Agent. *Bayl. Univ. Med. Cent. Proc.* **2003**, *16*, 241–248. [CrossRef]

70. Mertas, A.; Garbusińska, A.; Szliszka, E.; Jureczko, A.; Kowalska, M.; Król, W. The influence of tea tree oil (Melaleuca alternifolia) on fluconazole activity against fluconazole-resistant Candida albicans strains. *Biomed. Res. Int.* **2015**, *2015*, 590470. [CrossRef]
71. elsociova, S.; Kacaniova, M.; Horská, E.; Vukovic, N.; Hleba, L.; Petrová, J.; Rovná, K.; Stricik, M.; Hajduová, Z. Antifungal activity of essential oils against selected terverticillate penicillia. *Ann. Agric. Environ. Med.* **2015**, *22*, 38–42. [CrossRef]
72. Miron, D.; Battisti, F.; Silva, F.K.; Lana, A.D.; Pippi, B.; Casanova, B.; Gnoatto, S.; Fuentefria, A.; Mayorga, P.; Schapoval, E.E. Antifungal activity and mechanism of action of monoterpenes against dermatophytes and yeasts. *Rev. Bras. Farmacogn.* **2014**, *24*, 660–667. [CrossRef]
73. Sobrinho, A.C.N.; de Souza, E.B.; Marcos, F.; Albuquerque, M.R.J.R.; Bandera, P.N.; de Morais, S.M.; dos Santos Fontenelle, R.O.; de Paula Cavalcante, C.S. Cytotoxicity, antifungal and antioxidant activities of the essential oil from Eupatorium ballotifolium Kunth (Asteraceae). *Afr. J. Pharm. Pharmacol.* **2016**, *10*, 346–355.
74. Zhan, J.; He, F.; Cai, H.; Wu, M.; Xiao, Y.; Xiang, F.; Yang, Y.; Ye, C.; Wang, S.; Li, S. Composition and antifungal mechanism of essential oil from Chrysanthemum morifolium cv. Fubaiju. *J. Funct. Foods* **2021**, *87*, 104746. [CrossRef]
75. Taheri, P.; Soweizy, M.; Tarighi, S. Application of essential oils to control some important fungi and bacteria pathogenic on cereals. *J. Nat. Pestic. Res.* **2023**, *6*, 100052. [CrossRef]
76. Nazzaro, F.; Fratianni, F.; Coppola, R.; Feo, V. Essential oils and antifungal activity. *Pharmaceuticals* **2017**, *10*, 86. [CrossRef]
77. Hatice, K.; Bengü, E. Investigation of antifungal activity mechanisms of alpha-pinene, eugenol, and limonene. *J. VetBio Sci. Tech.* **2022**, *7*, 385–390.
78. Mustafa, K.H.; Khorshidi, J.; Vafaee, Y.; Rastegar, A.; Morshedloo, M.R.; Hossaini, S. Phytochemical profile and antifungal activity of essential oils obtained from different Mentha longifolia L. accessions growing wild in Iran and Iraq. *BMC Plant Biol.* **2024**, *24*, 461. [CrossRef]
79. da Cruz, R.P.; Castro, J.W.G.; Leite, D.O.D.; de Carvalho, N.K.G.; Almeida-Bezerra, J.W.; Pereira, R.L.S.; Rodrigues, F.F.G.; Bezerra, J.J.L.; Costa, A.R.; Mori, E.; et al. Chemical Composition and Antimicrobial Potential of Essential Oil of Acritopappus confertus (Gardner) R.M.King & H.Rob. (Asteraceae). *Pharmaceuticals* **2022**, *15*, 1275. [CrossRef]
80. Albayrak, G.; Yörük, E.; Teker, T.; Sefer, Ö. Investigation of antifungal activities of myrcene on Fusarium reference strains. *Arch. Microbiol.* **2023**, *205*, 82. [CrossRef]
81. Alighiri, D. Isolation and Antifungal Activity of Caryophyllene from Clove Leaf Oil (*Syzygium aromaticum* L.) on Mahogany Leaf Composites. *Sci. Community Pharm. J.* **2022**, *1*, 1–6.
82. Domingos, L.T.S.; Pereira, F.G.; Moraes, D.C.d.; Marquete, R.; Rocha, M.E.d.N.; Moreira, D.d.L.; Mansur, E.; Ferreira-Pereira, A. Casearia sylvestris essential oil and its fractions inhibit Candida albicans ABC transporters related to multidrug resistance (MDR). *Rodriguésia* **2020**, *72*, e00432020. [CrossRef]